Design and Fabrication of Temperature-Insensitive InGaP–InGaAlP Resonant-Cavity Light-Emitting Diodes

Yi-An Chang, Chun-Lung Yu, I-Tsung Wu, Hao-Chung Kuo, Tien-Chang Lu, Fang-I Lai, Li-Wen Laih, Li-Horng Laih, and Shing-Chung Wang

***Abstract*—Visible InGaP–InGaAlP resonant-cavity light-emitting diodes with low-temperature sensitivity output characteristics were demonstrated. By means of widening the resonant cavity to a thickness of three wavelength (3λ), the degree of power variation between 25 °C and 95 °C for the devices biased at 20 mA was apparently reduced from −2.1 dB for the standard structure design (1 − λ avity) to −0.6 dB. An output power of 2.4 mW was achieved at 70 mA. The external quantum efficiency achieved a maximum of 3% at 13 mA and dropped slowly with increased current for the device. The external quantum efficiency at 20 mA dropped only 14% with elevated temperature from 25 °C to 95 °C. The current dependent far-field patterns also showed that the emission always took place perfectly in the normal direction, which was suitable for plastic fiber data transmission.**

***Index Terms*—InGaAlP, light-emitting diode (LED), optical communication, optoelectronic device, resonant cavity.**

I. Introduction

RESEARCH progress of resonant-cavity light-emitting diodes (RCLEDs) has unmitigatedly continued to the present since the novel concept proposed by Schubert [1]. RCLEDs enjoy several advantages, including improved spectral purity, highly directional light output, less chromatic dispersion, and improved modulation bandwidth in comparison to typical light-emitting diodes. As compared with vertical-cavity surface-emitting lasers, the epitaxial complexity of RCLED structure is reduced since the reflectivity of upper distributed Bragg reflectors (DBRs) has to be less than 90%, and thus the RCLEDs provide thresholdless operation, less temperature dependence, and better fabrication reliability. RCLEDs with visible red emission are suitable candidates for short-distance data communication applications due to a minimum attenuation loss (0.1 dB/m) at 650 nm in the polymethyl methacrylate plastic optical fibers (POFs) [2]. Recently, the application of POFs has been extended to the automotive industry, such as media oriented systems transport, which needs to carrier 50–250 Mb/s of data over POFs. In an RCLED, the Fabry–Pérot cavity, sandwiched between upper and lower DBRs, is generally designed with $1-\lambda$ thickness, and the quantum wells (QWs) are embedded at the antinode of the standing wave cavity mode. The gain cavity detuning $(\Delta\lambda_{\mathrm{detuning}} = \lambda_{\mathrm{FP}} - \lambda_{\mathrm{qw}})$ is often designed to be positive to have a higher optical gain. Most importantly, to obtain better characteristics under high-temperature operation, the careful design of $\Delta\lambda_{\mathrm{detuning}}$ is required because the maximal modal gain red-shifts and matches the resonance dip as the device temperature increases. Hild *et al.* had reported the RCLEDs were less temperature-sensitive over the 15 °C–75 °C temperature range by a large gain cavity detuning [3]. However, the high-temperature output performance was still restricted by carrier leakage [3]–[5].

In the field of 650-nm RCLEDs, the researchers had reported a high output power of 8.4 mW operated at 120 mA with 202-μm device diameter [6], a peak external quantum efficiency of 10.2% for a large area device [7], low voltage operation [8], and high modulation bandwidth [9]–[12]. While most of the focus has been put on achieving high output characteristics under room-temperature (RT) operation and improving modulation bandwidth, the study of stabilizing output performance in RCLEDs with elevated device temperature and injection current is rare. Therefore, we report in this study the design and fabrication of temperature-insensitive InGaP–InGaAlP RCLEDs by means of widening the resonant cavity to 3λ, where the number of QWs is increased by a factor of three and the QWs are separated into three parts to reduce leakage current. As compared with the conventional RCLED of $1-\lambda$-cavity design, the temperature-dependent light output and voltage (*L–I–V*) characteristics, 3-dB modulation bandwidths, and far-field patterns are characterized and discussed.

II. Device Fabrication and Characteristics

In this study, the RCLED structures were grown by a low-pressure (50 torr) metal–organic chemical vapor deposition system on n-type GaAs (100) substrate. Methyl-organometallics, phosphine, and arsine were used as the sources for epitaxy. SiH_4 and CBr_4 were the n- and p-type dopants. A schematic plot of device structures is shown in Fig. 1. Two structures were prepared, in which the bottom DBR was identically comprised of 35 pairs of n-type quarter-wave $Al_{0.95}Ga_{0.05}As$–$Al_{0.5}Ga_{0.5}As$ layers for both devices to provide a $\sim$99% reflectivity, and the top DBRs was identically comprised of 7 pairs of p-type

Manuscript received March 13, 2006; revised April 20, 2006. This work was supported by the National Science Council under Grant NSC94-2752-E009-007-PAE and Grant NSC94-2120-M009-007.

Y.-A. Chang, H.-C. Kuo, T.-C. Lu, and S.-C. Wang are with Department of Photonics and Institute of Electro-Optical Engineering, National Chiao-Tung University, Hsinchu 300, Taiwan, R.O.C. (e-mail: hckuo@faculty.nctu.edu.tw).

C.-L. Yu, I.-T. Wu, and F.-I. Lai are with Department of Electrical Engineering, Ching Yung University, Jung-Li 320, Taiwan, R.O.C. (e-mail: filai@cyu.edu.tw).

L.-W. Laih and L.-H. Laih are with Millennium Communication Co., Hsinchu Industrial Park, 303 Taiwan, R.O.C. (e-mail: lwlaih@m-comm.com.tw).

Digital Object Identifier 10.1109/LPT.2006.879931

1041-1135/$20.00 © 2006 IEEE

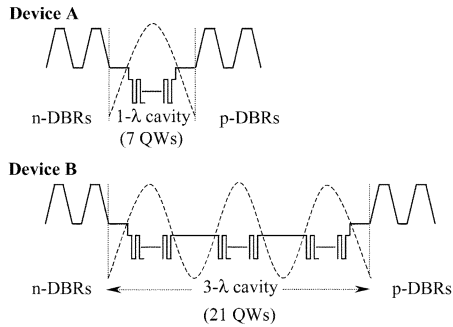

Fig. 1. Schematic plot of device structures. Device A was designed with a conventional $1-\lambda$ resonant cavity. Device B was designed to have a $3-\lambda$ resonant cavity, while the number of QWs was tripled and separated into three parts.

$Al_{0.95}Ga_{0.05}As$–$Al_{0.5}Ga_{0.5}As$ layers. A separate-confinement-heterostructure strained multiple quantum wells active region, which contains $In_{0.52}Ga_{0.48}P$ wells and $In_{0.5}(Ga_{0.5}Al_{0.5})_{0.5}P$ barriers, and $In_{0.5}(Ga_{0.3}Al_{0.7})_{0.5}P$ cladding layers formed the resonant cavity. For Device A, the cavity was standardized to 1λ and the cavity for Device B was widened to 3λ and the number of QWs was tripled. From mapping a 2-in epi-wafer, the QW photoluminescence (PL) emission of both devices was about 644 nm, and the Fabry–Pérot dip, determined from the reflection measurement was in a range of 650–656 nm. The doping levels of n- and p-type DBRs, determined from electrochemical CV profiling (ECV) measurement, were 2×10^{18} and 4×10^{18} cm^{-3}. After epitaxial growth, standard fabrication processes, including photolithography, implantation, metallization, and bonding techniques, were used so as to fabricate the devices with surface emission. The light extraction window of both devices in this study was 80 μm in diameter. The RCLED chips were mounted onto TO-46 headers and the chip size was in 250×250 μm^2 square.

The direct current characteristics of RCLEDs were measured using a Keithly 238 current source, a Newport 1835C power meter module, and an Advantec optical spectrum analyzer with a 0.1-nm spectral resolution. As a result of Joule heating, the peak emission wavelength increased with increased bias current at a red shift of 0.083 nm/mA for Device A, 0.082 nm/mA for Device B, and the devices exhibited a peak of 656.8 and 659.4 nm when the bias current was 40 mA, respectively. Temperature-dependent *L–I–V* characteristics of Devices A and B are shown in Fig. 2. The highly C-doped p-type DBRs and high-quality ohmic contacts resulted in a low operating voltage of 2.1 V at a current of 20 mA in Device A, while the thicker undoped cavity in Device B gave a higher voltage of 2.37 V at 20 mA. An output power of 1.9 mW in Device A at 20 mA under RT operation was achieved, and it reached a maximum of 3.1-mW output when the device was biased at 57 mA. For Device B, even though the output power at low current was not higher than that in Device A, the output characteristic was stable, which indicated that the temperature effect on Device B was much less sensitive. The power variation between 25 °C and 95 °C for Devices A and B at 20 mA were approximately −2.1 and −0.6 dB. We suppose that the improved stable output performance under high current injection and high-temperature operation in Device B is from the increased number of QWs that decreases the carrier leakage.

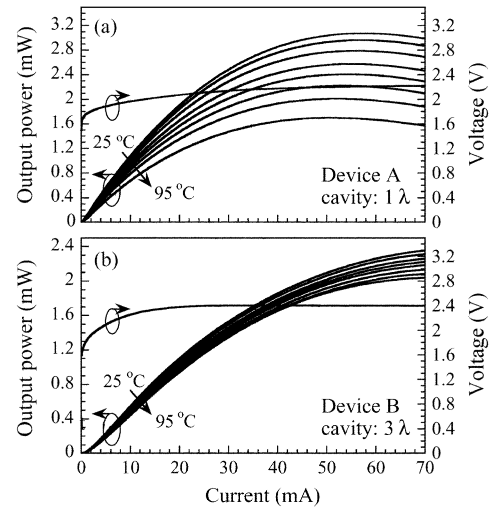

Fig. 2. Temperature-dependent *L–I–V* characteristic of (a) Device A and (b) Device B. The curve was obtained in a device temperature range of 25 °C–95 °C.

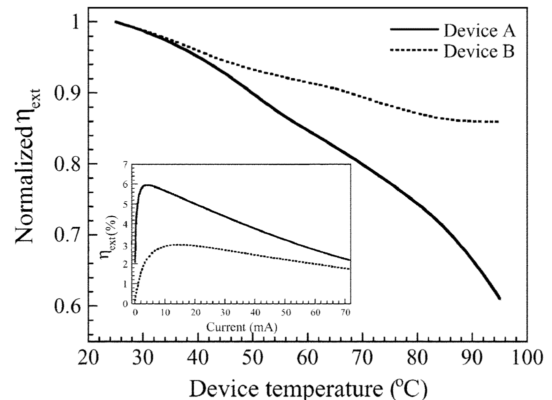

Fig. 3. Normalized external quantum efficiency ($\eta_{\rm ext}$) value obtained at 20 mA with elevated device temperature from 25 °C to 95 °C. The inset was the $\eta_{\rm ext}$ value versus current at RT for both devices.

The temperature-dependent external quantum efficiency ($\eta_{\rm ext}$) normalized to the value obtained at 20 mA is depicted in Fig. 3. The inset shows the $\eta_{\rm ext}$ value versus current at RT. For Device A, a maximum $\eta_{\rm ext}$ value of 6% was achieved when the device was biased at 5.8 mA. As shown in previous studies, the highest $\eta_{\rm ext}$ value of RCLEDs was often obtained at a low current level, typically less than 10 mA, and consequently decreased at higher current levels by internal heating effect. In red emitting devices, this phenomenon is more serious because the conduction band offset value in InGaP–InGaAlP material is relatively low compared to the InGaN–GaN and AlGaAs–GaAs materials [13], [14]. The increased device temperature at higher current level will induce more leakage current, resulting in less radiative recombination, and therefore, decreases the output performance. To reduce the induced leakage current at high current level injection and under high temperature operation, the resonant cavity in Device B was increased to 3λ and the number of QWs was tripled simultaneously, which was a direct way to confine more carriers in the QWs of the resonant cavity. This approach should be effective since the normalized $\eta_{\rm ext}$ value for Device B dropped only 14% with elevated device temperature to 95 °C. In addition, the decrease of $\eta_{\rm ext}$ at high

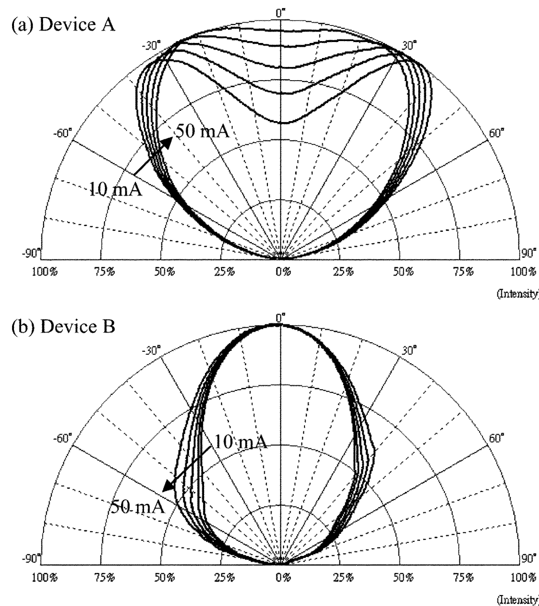

Fig. 4. Evolution of far-field patterns for both devices under RT operation with increased bias current of 10–50 mA. The slightly unsymmetrical patterns could be attributed to the TO package.

current levels, shown in the inset of Fig. 3, was also less pronounced. The lower η_{ext} for Device B than for Device A might be because the number of QWs was tripled which induced more absorption in QWs, and a less optimally tuned cavity due to the thicker emission region. Dynamic properties of the RCLED devices were studied by using a calibrated vector network analyzer (Agilent 8720ES) and 50-μm multimode optical fiber connected to a Si photodetector. A light extraction window diameter of 80 μm was used for POF-based communication. However, there is a tradeoff between light extraction output power and small signal 3-dB frequency bandwidth ($f_{-3\ \text{dB}}$). A smaller light extraction window diameter will bring on a lower capacitance, resulting in the decreased resistance capacitance (*RC*) time constant, but a weak output power performance. In our devices, the $f_{-3\ \text{dB}}$ value was found to increase with increased bias current with a slope of 0.44 MHz/mA for Device A, 0.2 MHz/mA for Device B, and achieved to a maximum of 116, and 87 MHz at 70 mA, respectively. The lower $f_{-3\ \text{dB}}$ value for Device B than for Device A might be attributed to that the number of QWs is tripled. Hence, the current density in each QW of the Device B may be relatively lower than that of the Device A. In addition, the thicker resonant cavity might cause the increase of series resistance that reduced the $f_{-3\ \text{dB}}$ value. Further minimization of the capacitance at the pn junction and adjustment of the bonding pad to reduce the parasitic capacitance will be required.

The evolution of far-field patterns under RT with increased bias current of 10–50 mA is shown in Fig. 4. For Device A, the emission took place at the angle of $\pm 33°$, and the angle became $\pm 20°$ when the device was biased at 50 mA. Narrowing far-field angle is undoubtedly required under the consideration of fiber coupling efficiency. In conventional $1-\lambda$-cavity RCLEDs, while increasing bias current can narrow the far-field emission angle, the output power often rolls over at high current level injection. By widening the resonant cavity to 3λ, we found that the angle of the lobe was zero and the small divergence angle of the far-field pattern remained almost unchanged over the entire measured bias current range.

III. Conclusion

In summary, we have fabricated visible InGaP–InGaAlP RCLEDs with low-temperature sensitivity of the output performance. By widening the resonant cavity to 3λ, the degree of power variation was apparently reduced to -0.6 dB, and the η_{ext} value dropped only 14.1% when the device was biased at 20 mA with elevated temperature from 25 °C to 95 °C. The current dependent far-field patterns also showed that the emission of the $3-\lambda$ RCLEDs always took place perfectly in the normal direction. The results indicate the $3-\lambda$ RCLEDs can provide stable output characteristics and are suitable for data communication applications.

References

[1] E. F. Schubert, Y.-H. Wang, A. Y. Cho, L.-W. Tu, and G. J. Zydzik, “Resonant cavity light-enitting diode,” *Appl. Phys. Lett.*, vol. 60, no. 8, pp. 921–923, 1992.

[2] T. Ishigure, M. Satoh, O. Takanashi, E. Nihei, T. Nyu, S. Yamazaki, and Y. Koike, “Formation of the refractive index profile in the graded index polymer optical fiber for gigabit data transmission,” *J. Lightw. Technol.*, vol. 15, no. 11, pp. 2095–2100, Nov. 1997.

[3] K. Hild, T. E. Sale, T. J. C. Hosea, M. Hirotana, Y. Mizuno, and T. Kato, “Spectral and thermal properties of red AlGaInP RCLEDs for polymer optical fibra applications,” in *Proc. Inst. Elect. Eng., Optoelectron.*, 2001, vol. 148, no. 5/6, pp. 220–224.

[4] A. I. Onischenko, T. E. Sale, E. P. O’Reilly, A. R. Adams, S. M. Pinches, J. E. F. Frost, and J. Woodhead, “Progress in the design and development of AlGaInP visible VCSELs,” in *Proc. Inst. Elect. Eng., Optoelectron.*, 2000, vol. 147, no. 1, pp. 15–21.

[5] K. Streubel, N. Linder, R. Wirth, and A. Jaeger, “High brightness AlGaInP light-emitting diodes,” *IEEE J. Sel. Topics Quantum Electron.*, vol. 8, no. 2, pp. 321–332, Mar./Apr. 2002.

[6] K. Streubel, U. Helin, V. Oskarsson, E. Bäcklin, and Å. Johansson, “High brightness visible (660 nm) resonant-cavity light-emitting diode,” *IEEE Photon. Technol. Lett.*, vol. 10, no. 12, pp. 1685–1687, Oct. 1998.

[7] R. Wirth, C. Karnutsch, S. Kugler, and K. Streubel, “High efficency resonant-cavity LEDs emitting at 650 nm,” *IEEE Photon. Technol. Lett.*, vol. 13, no. 5, pp. 421–423, May 2001.

[8] J. W. Gray, Y. S. Jalili, P. N. Stavrinou, M. Whitehead, G. Parry, A. Joel, R. Robjohn, R. Petrie, S. Hunjan, P. Gong, and G. Duggan, “High-efficiency, low voltage resonant-cavity light-emitting diodes operating around 650 nm,” *Electron. Lett.*, vol. 36, no. 20, pp. 1730–1731, 2000.

[9] P. Sipilä, M. Saarinen, M. Guina, V. Vilokkinen, M. Toivonen, and M. Pessa, “Temperature behaviour of resonant cavity light-emitting diodes at 650 nm,” *Semicond. Sci. Technol.*, vol. 15, pp. 418–421, 2000.

[10] E. F. Schubert, N. E. J. Hunt, R. J. Malik, M. Micovic, and D. L. Miller, “Temperature and modulation characteristics of resonant-cavity light-emitting diodes,” *J. Lightw. Technol.*, vol. 14, no. 7, pp. 1721–1729, Jul. 1996.

[11] M. Guina, S. Orsila, M. Dumitrescu, M. Saarinen, P. Sipilä, V. Vilokkinen, B. Roycroft, P. Uusimaa, M. Toivonen, and M. Pessa, “Light-emitting diode emitting at 650 nm with 200-MHz small-signal modulation bandwidth,” *IEEE Photon. Technol. Lett.*, vol. 12, no. 7, pp. 786–788, Jul. 2000.

[12] C.-L. Tsai, C.-W. Ho, C.-Y. Huang, F.-M. Lee, M.-C. Wu, H.-L. Wang, S.-C. Ko, W.-J. Ho, J. Huang, and J. R. Deng, “Fabrication and characterization of 650 nm resonant-cavity light-emitting diodes,” *J. Vac. Sci. Technol. B*, vol. 22, no. 5, pp. 2518–2521, 2004.

[13] D. P. Bour, R. S. Geels, D. W. Treat, D. L. Paoli, F. Ponce, R. L. Thomton, B. S. Krusor, R. D. Bringans, and D. F. Welch, “Strained $\text{Ga}_x\text{In}_{1-x}\text{P}/(\text{AlGa})_{0.5}\text{In}_{0.5}\text{P}$ heterostructures and quantum-well laser diodes,” *IEEE J. Quantum Electron.*, vol. 30, no. 2, pp. 593–607, Feb. 1994.

[14] K. Interholzinger, D. Patel, C. S. Menoni, P. Thiagarajan, G. Y. Robinson, and J. E. Fouquet, “Strain-induced modifications of the band structure of $\text{In}_x\text{Ga}_{1-x}\text{P-In}_{0.5}\text{Al}_{0.5}\text{P}$ multiple quantum wells,” *IEEE J. Quantum Electron.*, vol. 34, no. 1, pp. 93–100, Jan. 1993.